



Title	Physical hydrogels composed of polyampholytes demonstrate high toughness and viscoelasticity
Author(s)	Sun, Tao Lin; Kurokawa, Takayuki; Kuroda, Shinya; Bin Ihsan, Abu; Akasaki, Taigo; Sato, Koshiro; Haque, Md Anamul; Nakajima, Tasuku; Gong, Jian Ping
Citation	Nature materials, 12(10), 932-937 <a href="https://doi.org/10.1038/NMAT3713">https://doi.org/10.1038/NMAT3713</a>
Issue Date	2013-10
Doc URL	<a href="http://hdl.handle.net/2115/56662">http://hdl.handle.net/2115/56662</a>
Rights(URL)	<a href="http://www.nature.com/authors/policies/license.html">http://www.nature.com/authors/policies/license.html</a>
Type	article (author version)
Additional Information	There are other files related to this item in HUSCAP. Check the above URL.
File Information	Gong-Manuscript-1.pdf



[Instructions for use](#)

**Physical hydrogels composed of polyampholytes demonstrate  
high toughness and viscoelasticity**

Tao Lin Sun<sup>1†</sup>, Takayuki Kurokawa<sup>2†</sup>, Shinya Kuroda<sup>1</sup>, Abu Bin Ihsan<sup>3</sup>,  
Taigo Akasaki<sup>3</sup>, Koshiro Sato<sup>3</sup>, Md. Anamul Haque<sup>2</sup>, Tasuku Nakajima<sup>2</sup>, Jian Ping Gong<sup>2\*</sup>

<sup>1</sup>Graduate School of Science, Hokkaido University, Sapporo 060-0810, Japan

<sup>2</sup>Faculty of Advanced Life Science, Hokkaido University, Sapporo 060-0810, Japan

<sup>3</sup>Graduate School of Life Science, Hokkaido University, Sapporo 060-0810, Japan

<sup>†</sup>These authors contributed equally to this work.

\*E-mail: [gong@mail.sci.hokudai.ac.jp](mailto:gong@mail.sci.hokudai.ac.jp)

**Hydrogels draw great attention as biomaterials due to their soft and wet nature similar to biotissues. Recent inventions of several tough hydrogels show their high potential as structural biomaterials, such as cartilage. However, any given application requires a combination of mechanical properties including the stiffness, strength, toughness, damping, fatigue resistance, self-healing, along with biocompatibility, which are rarely realized. We report that polyampholytes, polymers bearing randomly dispersed cationic and anionic repeat groups, form tough and viscoelastic hydrogels with multiple mechanical properties. The randomness makes ionic bonds of a wide distribution of strength. The strong bonds serve as permanent crosslinks, imparting the elasticity, while the weak bonds reversibly break and re-form, dissipating energy. These physical hydrogels of supramolecular structure can be tuned to change multiple mechanical properties over wide ranges by using diverse ionic combinations. This polyampholyte approach is simple in synthesis and largely increases the choice of tough hydrogels for applications.**

Hydrogels draw great attention as biomaterials due to their soft and wet nature similar to biotissues<sup>1-3</sup>. Previously they were considered as a class of mechanically weak materials, and thus little attention was paid to them as possible structural materials<sup>4-6</sup>. Recent inventions of several tough hydrogels show their high potential as structural biomaterials, such as cartilage<sup>7-9</sup>. Any given applications as load-bearing materials require a combination of mechanical properties including the stiffness, strength, fatigue resistance, damping, self-healing, in addition to a high toughness<sup>2,3,10,11</sup>. For example, cartilage substitute materials require a relatively high stiffness (~ MPa) and mouth guard materials require relatively low stiffness and high shock-absorbing ability, in addition to high strength and toughness. Smart structural materials in surgery, such as guide wires of catheter, require shape memory properties. Synthesis of novel hydrogel materials with these multiple mechanical properties are currently the great aim in the field.

Studies on double network (DN) hydrogel, an extraordinarily tough hydrogel consisting of interpenetrating brittle and ductile networks, has clarified that the toughness is due to the internal

fracturing of the brittle network, which effectively dissipates energy and prevents catastrophic crack propagation upon loading<sup>12-14</sup>. The double-network concept revealed a novel principle of the toughness, that is, *the existence of an easily fractured, brittle internal structure makes the material as a whole mechanically tough*. Thus, the brittle network acts as a ‘sacrificial bond’, a term originally used to describe the toughening of bones<sup>15</sup>. This principle naturally suggests a new strategy for designing high-strength materials: incorporating, on purpose, a mechanically fragile structure to toughen the material as a whole. Since the rupture of the brittle network causes permanent damage, a DN gel softens and does not recover after experiencing large deformation. To address this problem, several recent works have replaced the covalent bonds with non-covalent bonds to allow the fractured bond to be reformed<sup>16-18</sup>. Studies along these lines have successfully produced tough hydrogels with partial or full self-recovery after internal rupture. For example, a very soft and stretchable DN-type hydrogel has recently been synthesized by using metal ion cross-linked alginate as the sacrificial network<sup>18</sup>.

In this study, we present a novel class of tough and viscoelastic hydrogels from polyampholytes that can be tuned to change multiple mechanical properties over wide ranges. These physical polyampholyte hydrogels are synthesized by random copolymerization of oppositely charged ionic monomers around the charge balance point at high concentration. The randomness of charges forms multiple ionic bonds with a wide distribution of strengths, via inter and intra chain complexation. The ionic bonds play two roles for the mechanical properties of the hydrogels: as strong bonds and weak bonds, different from other hydrogels in which they are used as weak bonds<sup>16,18</sup>. The strong bonds serve as permanent crosslinks to maintain the shape of the gel, while the weak bonds perform several mechanical functions simultaneously: enhance the fracture resistance by bond rupture and therefore toughen the materials, enhance the shock absorb by generating high internal friction, enhance the fatigue resistance and self-healing by bond reformation. Accordingly, the physical polyampholyte hydrogels become tough in analogy to double-network hydrogels though they have different topological structure: the strong bonds form primary network and the weak bonds form sacrificial network.

As all the ion groups form ion bonds, the polyampholyte gels have a supramolecular structure, and contain 50-70 wt% of water at an equilibrium state, which is much less than that of conventional hydrogels that usually have high water content (> 80 wt%). They are strongly viscoelastic and have a high toughness (fracture energy of 4000 J/m<sup>2</sup>), 100% self-recovery, and high fatigue resistance. Some gels showed partial self-healing after cutting and solvent-induced shape memory effect. Young’s modulus and damping ability can be tuned over a wide range by choosing the proper ion combination. In addition, they are non-toxic and anti-fouling to cell adhesion. Many studies on the properties of polyampholytes, both the solution and the chemically crosslinked hydrogels, have been reported<sup>19-23</sup>. This is the first report on the possibility of polyampholytes as structural biomaterials. This polyampholyte approach has large advantages for practical applications of hydrogels: it is general and directly applicable to a variety of ionic monomer combinations with specific functions; it

largely increases the choices of tough hydrogels with desirable combinations of mechanical properties; the one-step polymerization process is easy to scale-up for mass production.

### ***Formulation for tough physical hydrogel***

To obtain weak bond that can sustain a load during the initial deformation but ruptures preferentially before the rupture of covalent bonds of the polymer chains, the ionic association energy  $E_{ion}$  should be higher than the thermal energy  $k_B T$  (room temperature) but much lower than the covalent bond dissociation energy  $E_{c-c} \sim 347$  kJ/mol ( $140 k_B T$ )<sup>24</sup>. Since the bond energy of one ionic pair in water is  $\sim k_B T$  at room temperature<sup>25</sup>, multiple ion bonds of several to decades of ion pairs is required at room temperature (Fig. 1a). On the other hand, the strong bonds should consist of decades to a hundred of ion pairs. We demonstrate that such structures can be obtained simply by synthesizing the hydrogel from a very concentrated aqueous solution of oppositely charged monomers at charge ratio near 1:1.

As one typical example of such a synthesis, we used a pair of ionic monomers, sodium *p*-styrenesulfonate (NaSS) and 3-(methacryloylamino)propyl-trimethylammonium chloride (MPTC) (Fig. 1b). We confirmed that this system forms random polymers (Supplementary Fig. 1).

To obtain hydrogels, we should synthesize the sample near the charge balance at high concentration. The charge balance condition is required since the Coulomb attraction prevails over the repulsion for neutral polyampholytes and the polymers collapse to a globule state<sup>19,20</sup>. The high concentration condition is required to prevent phase separation. In this specific system, the charge balance point is at the molar fraction of the anionic monomer  $f = 0.52$ , which can be simply determined from the maximum deswelling of their chemically crosslinked hydrogels (Supplementary Fig. 2 and Table 1). So we fix at  $f = 0.52$  and synthesize polyampholytes with different monomer concentration,  $C_m$ . Hereafter, we denote the samples using the code  $C_m$ - $f$  after the names of the copolymers, where  $C_m$  (M) is the total molar concentration of ionic monomers, and  $f$  is the molar fraction of anion.

When  $C_m$  is low, precipitation or phase separation occurs, in agreement with the previous studies<sup>19,20</sup>. When  $C_m$  is high enough ( $C_m = 0.8$ - $2.2$  M), we obtain uniform hydrogel phase, either turbid or transparent (Fig. 2a). These gels swell ( $Q_v = V/V_0 > 1$ ) at  $C_m < 1.6$  M and shrink ( $Q_v < 1$ ) at  $C_m > 1.6$  M, but never dissolve in water (Fig. 2b). Here  $V$  and  $V_0$  are volumes of gels equilibrated in water and at the as-prepared state, respectively.  $Q_v$  values of the gels reach a constant at  $C_m > 1.6$  M. In corresponding to this, the modulus of the gels,  $E$ , increases with  $C_m$  and also reach constant at  $C_m > 1.6$  M. This indicates that the electrostatic attraction between the polymer chains is stabilized at high concentration to form a stable supramolecular hydrogel even without chemical cross-linking. It is confirmed that there is no any covalent crosslinking in the gels as they dissolve completely in 4 M NaCl solutions at high temperature ( $> 50^\circ\text{C}$ ) after 2 days. The strong concentration effect on the gelation is attributed to the entanglement of polymers. A rough estimation of the entanglement concentration from the molecular weight of the sample P(NaSS-co-MPTC) 2.1-0.52 supports this argument (“Molecular weight” in Supplementary Information). The fact that the critical  $C_m$  of gelation shifted to a lower value when adding a small amount of chemical crosslinker also supports

this argument (data not shown).

During the shrinking process of the as-prepared sample in pure water, the mobile counter-ions are dialyzed away from the hydrogel, which substantially stabilizes both the intra- and interchain ionic complexes to form a tough hydrogel (Supplementary Fig. 3a). The as-prepared gel was very soft and elastic, and it showed no residual strain after deformation. These results indicate that some strong bonds are already formed in the as-prepared state. On the other hand, the gel in water became much more rigid, showing clear yielding and large hysteresis (Supplementary Fig. 3b). The latter two features are characteristic of tough materials.

The tensile stress-strain curves of the gels in Fig. 2c demonstrate that increases in  $C_m$  remarkably enhance the mechanical performance. The gels synthesized at low monomer concentrations ( $C_m \sim 1.3$  M) do not show any yielding point, indicating weak ionic association, while the gels synthesized at high concentrations ( $C_m > 1.5$  M) exhibit clear yielding points with dramatically enhanced fracture stress  $\sigma_b$  and strain  $\varepsilon_b$  values that reach as high as 1.8 MPa and 750%, respectively. Apparently, the enhanced mechanical strength is due to the strong ion bonds formation at elevated concentration, and the distinct yielding observed beyond a certain strain stems from the internal rupture of the ion complex. The fracture stress  $\sigma_b$  scales with the weight fraction of polymers  $C_{poly}$  of the gels, as  $\sigma_b \sim C_{poly}^{1.7}$  (Fig. 2d). The tearing energy  $T$ , a direct measure of the resistance to crack propagation or toughness, of the gels also follows a scaling relation with  $C_{poly}$ ,  $T \sim C_{poly}^{1.8}$  and can reach a value as high as 4000 J/m<sup>2</sup> (Fig. 2d). These scaling relations can be quantitatively explained by an ionic interaction model (Supplementary Fig. 4).

A large yielding zone was observed around the crack tip using a polarized optical microscope (inset image of Fig. 2d), indicating that these zones toughen the material in a similar way to the damage zone in a DN gel<sup>12,26</sup> or the crazing zone in rubber-like materials<sup>27</sup> in terms of blunting and energy dissipation.

### ***Hysteresis, self-recovery, fatigue resistance, and self-healing***

The hydrogels show 100% self-recovery and therefore have very high fatigue resistance. As shown in Fig. 3a, distinct yielding and large hysteresis are observed for the first loading-unloading cycle of P(NaSS-co-MPTC) 2.1-0.52. However, the stress-strain curve completely recovers to the original loading curve after a relatively short waiting time ( $\sim 120$  min). The waiting time dependence of the residual strain and the hysteresis ratio estimated from the hysteresis area change (Fig. 3b) indicate that the recovery involves both a quick process and a slow process. Similar phenomenon was observed in ionomers but with much longer recovery times<sup>28</sup>. This two-stage recovery process is probably related to the competition between the elasticity of primary chain and the strength of temporarily reformed bonds during the unloading process. At large deformation (strain  $> 1.75$ ) the elastic contraction is dominant, which ruptures the reformed bonds and leads to quick recovery. At small deformation (strain  $< 1.75$ ) the elastic contraction becomes weak and the reformed bonds slow down the recovery of the primary chains to its equilibrium state. The slow process probably also

includes the re-organizing of the reformed bonds. The complete self-recovery, without residual strain, is observed up to a loading strain of 600%, which is close to the fracture strain of 700–800%. Therefore, even without covalent cross-linking, no chain sliding occurs under the large deformation in these gels. This behaviour is different from that of the various reported ionically cross-linked hydrogels, which show permanent residual strain due to the damage of the primary network<sup>16,18</sup>.

Because of its self-recovery ability, the gel has high fatigue resistance against repeated deformation, as shown by the cyclic tests performed with different loading strains (Fig. 3c). The hysteresis loops are the same for all the cycles, indicating fatigue-free behaviour. The gels show partial self-healing in salt solution or at an elevated temperature in water. As illustrated in Fig. 3d, if we cut two disc-shaped P(NaSS-co-MPTC) 2.1-0.52 samples dyed red and blue (Fig. 3d(1)) into half-moon pieces (Fig. 3d(2)) and then pressed the cut surfaces of the red and blue pieces together in hot water (50 °C), they merged together within several minutes (Fig. 3d(3)). The healing efficiency, defined as the ratio between the work required to break the healing joint and that required to break the virgin sample by tensile deformation, reached ~ 30% after 1 hour healing. The healed joint was able to withstand a very large stress. For example, a ribbon of virgin sample with a 5.2 mm<sup>2</sup> cross section is able to sustain a large load of up to 2 kgf, while the repaired sample can still sustain 0.2 kgf (Fig. 3e and Supplementary Movies 1 and 2). Furthermore, adhesion between uncut surfaces was also observed.

The gel also shows solvent-induced shape memory behaviour by rupture of weak bonds in NaCl solution (Supplementary Fig. 5 and Movie 3) and reforming in water.

### ***Other charge combinations and the chemical structure effect***

This polyampholyte approach is applicable to various ionic monomer combinations, where the ionic structure plays an important role. More examples of polyampholyte gels with different ion pair structures (Supplementary Fig. 6) are summarized in Supplementary Table 2. Tough polyampholyte gels are only formed from relatively bulky and hydrophobic ion combinations, and the mechanical properties of the gels strongly depend on the chemical structure. For example, the combination of NaSS and DMAEA-Q forms gels, while no gel is formed from the hydrophilic combination of anionic AMPS and cationic DMAEA-Q (Fig. 1b).

These polyampholyte hydrogels have a Young's modulus ranging from 0.01 to 8 MPa, bridging the gap between the conventional elastic hydrogels and soft tissues or rubbers<sup>6,29,30,31</sup>. More hydrophilic monomers produced softer gels. For example, the gel P(NaSS-co-MPTC) 2.0-0.52 is relatively rigid, with a modulus of 2.2 MPa. When the cationic monomer is changed from MPTC to the relatively less hydrophobic DMAEA-Q (Fig. 1b), the gel P(NaSS-co-DMAEA-Q) 2.0-0.52 is much softer, with a modulus of 0.1 MPa (Supplementary Fig. 7). The latter has a higher self-healing efficiency (~ 99%, Fig. 3f) and a stronger shock-absorbance ratio than the former (Supplementary Table 2). These differences could not be explained by the water content of the polyampholyte gels. As shown in the Supplementary Table 2, the more hydrophobic P(NaSS-co-MPTC) forms robust gels with a slightly

higher water content, while the less hydrophobic P(NaSS-co-DMAEA-Q) forms soft gels with less water content. The flexibility of the main chain or specific packing structure should also play a role in the swelling ratio. The relatively high flexibility can result in the tight packing structure and low swelling ratio.

Regardless of the modulus change, the polyampholyte gels are very strong and tough. They show tensile fracture stress  $\sigma_b = 0.1\text{--}2$  MPa, fracture strain  $\varepsilon_b = 150\%\text{--}1500\%$ , and work of extension at fracture  $W_b = 0.1\text{--}7$  MJ/m<sup>3</sup>. The latter is at least two orders of magnitude larger than that of a conventional hydrogel with the same water content and is comparable to that of a tough DN hydrogel. The polyampholyte gels show tearing energy of  $T = 1000\text{--}4000$  J/m<sup>2</sup>, comparable to those of tough DN hydrogels, soft tissues, and filled rubbers (Fig. 2d and Supplementary Table 2)<sup>6,29,30,31</sup>.

In contrast to the DN hydrogels, which are almost purely elastic due to a high water content of 90 wt%, these polyampholyte gels, due to their supramolecular structure with relatively low equilibrium water contents of 50-70 wt%, are strongly viscoelastic, showing high loss factor values  $\tan\delta$  and high shock-absorption values (Supplementary Table 2, Movies 4 and 5).

### ***Universality as Supramolecular Materials***

The polyampholyte hydrogels are amorphous in structure, as confirmed by wide angle X-ray scattering (WAXS) and differential scanning calorimetry (DSC) results (Supplementary Fig. 8). They have some features similar to those of glassy polymers: for example, they have a softening temperature  $T_s$  in the range of 0–100 °C that depends on the chemical structure of the ions (Supplementary Fig. 6 and Table 2). In particular, the more hydrophobic gel P(NaSS-co-MPTC) 2.1-0.52 has  $T_s \sim 48.2$  °C, above room temperature, while the less hydrophobic supramolecular gel P(NaSS-co-DMAEA-Q) 2.0-0.52 shows  $T_s \sim 17.3$ °C, below room temperature. Thus,  $T_s$  is an index that reflects the strength and stability of the ion complex of the hydrogels, and the different behaviours of the gels (Supplementary Fig. 7c) can be universally understood from whether their  $T_s$  is above (P(NaSS-co-MPTC)) or below (P(NaSS-co-DMAEA-Q)) room temperature. Furthermore, the dynamic behaviours of the gels at different temperatures and frequencies follow the principle of time-temperature superposition well (Supplementary Fig. 9). The constructed master curves exhibit *extremely* broad viscoelastic peaks (Supplementary Fig. 9a), which confirms that the gels have a wide distribution of ion complex structures. This is also confirmed by the wide distribution of the apparent activation energy  $E_a$  (Supplementary Fig. 9b). For example, the  $E_a$  of gel P(NaSS-co-MPTC) 2.1-0.52 is 71–308 kJ/mol. The low limit is about  $29 k_B T$ , and the high limit is close to the main chain C-C bond dissociation energy,  $E_{c-c} \sim 347$  kJ/mol. This guarantees the preferential rupture of the weak bonds and the maintaining of strong bonds under deformation. This argument is consistent with the behavior of the gels P(NaSS-co-MPTC) 2.1-0.525 in NaCl solution shown in Fig. 4. In low saline solution ( $C_{NaCl} \leq 0.15$  M), the weakest bonds rupture, as shown by the slight swelling ( $Q_{salt,water} = V_{salt}/V_{water} < 1.2$ ) and the dramatic decrease of Young's modulus  $E$  (from 1.53 to 0.37 MPa) and fracture stress  $\sigma_b$  (from 2.60 to 1.02 MPa), while the undisturbed strong bonds constraints the

deformation  $\varepsilon_b$  ( $\sim 940\%$ ). Addition of more salts ( $C_{NaCl}$ : 0.3  $\sim$  1.0 M) destroys the relatively strong bonds, leading to the enhanced swelling ( $Q_{salt,water} \sim 2.7$ ) and elongation of the gels ( $\varepsilon_b \sim 1800\%$ ). Meanwhile, the Young's modulus and fracture stress continue to fall due to the rupture of ionic bonds ( $E \sim 0.0037\text{MPa}$ ,  $\sigma_b \sim 0.07\text{MPa}$ ). Furthermore, the deformation-rate dependence of tensile behaviour (Fig. 4c) also confirms the physical picture described above. The dramatic increase in strength of the sample with the deformation-rate increase indicates the dynamic and reversible features of less stable weak bonds within the entire deformation rate range (Fig. 4d), whose features are absent in DN hydrogels<sup>12</sup>. This viscoelastic feature contributes to the high shock-absorption ratio and toughness of the hydrogels. It is noted that, the fracture strain is constant ( $\varepsilon_b \sim 1000\%$ , Fig. 4d), independent of the deformation-rate up to a sufficient high rate (400 mm/min). This indicates that few strong bonds rupture before the fully breakage of weak bonds, which is in consistent with the results in salt solution (Fig. 4b).

However, strong bonds prevents the self-healing process, which explains why the more hydrophobic system P(NaSS-co-MPTC) 2.1-0.52 shows a relatively poor self-healing efficiency ( $\sim 30\%$ ) while the less hydrophobic system P(NaSS-co-DMAEA-Q) 2.0-0.52 has a very high self-healing efficiency ( $\sim 99\%$ ) (Fig. 3f). The latter system has a narrower activation energy range ( $E_a = 112\text{--}248$  kJ/mol) and lower high-limit value of  $E_a$  than those of the former system. Both the strength and quantity of strong bonds should influence the self-healing.

To the author's knowledge, the previous supramolecule hydrogels, though showed the feature of the reversible bonds, such as self-healing ability, are mechanically not tough<sup>32-34</sup>. These polyampholyte hydrogels are the first example to demonstrate that the supramolecule structure can make a hydrogel tough, like the other reported supramolecular materials that have shown excellent mechanical properties<sup>35</sup>. As revealed in the present study, a requirement for toughness is the existence of high density weak bonds and a good balance with strong bonds, which are probably lacked in the previously reported supramolecular hydrogels. Along this line, novel tough supramolecular hydrogels based on hydrogen bond, hydrophobic interaction, and so on, are expected to be produced. These polyampholyte hydrogels have excellent biocompatibility and anti-biofouling properties, as confirmed by the cytotoxicity test (Supplementary Fig. 10 and Table 3) and adhesion test using macrophages that are highly adhesive cells responsible for immune response to implant materials (Supplementary Fig. 11). As the materials have a wide spectrum of excellent mechanical properties even in physiological solutions, they have high potential as structural biomaterials. Also, the anti-biofouling property suggests the potential use in hygiene and medical fields.

### **Methods Summary**

Polyampholyte hydrogels were synthesized using the one-step random copolymerization of an anionic monomer and a cationic monomer. A mixed aqueous solution with the prescribed monomer concentration  $C_m$  and molar fraction  $f$  of the anionic monomer, 0.25 mol% UV initiator, 2-oxoglutaric acid (in a concentration relative to the total monomer concentration  $C_m$ ), and 0.5 M NaCl was poured



into in a reaction cell consisting of a pair of glass plates and irradiated with 365 nm UV light for 11 hours. After polymerization, the as-prepared gel was immersed in a large amount of water for 1 week to allow the gel to equilibrate and to wash away the residual chemicals. The water content of the equilibrated gels was measured by a freeze-drying process.

The tensile stress-strain measurements were performed using a tensile-compressive tester at a deformation rate of 100mm/min in air (Supplementary Fig. 12). Both the tearing test and pure shear test were performed in air to characterize the toughness of the sample, following the method established in references 18, 36 and 37 (Supplementary Figs. 13 and 14). The shock absorbance ratio was characterized using an impact tester. Rheological tests were performed using a commercial rheometer. In order to observe the stress concentration during the crack growth, the crack microstructure was frozen using acetone to avoid any stress relaxation, and then the sample was observed using polarized optical microscopy.

Further details on the methods are available in the Supplementary information.

## References

1. Yasuda, K. *et al.* A novel double-network hydrogel induces spontaneous articular cartilage regeneration in vivo in a large osteochondral defect. *Macromol. Biosci.* **9**, 307-316 (2009).
2. Drury, J. L. & Mooney, D. J. Hydrogels for tissue engineering: scaffold design variables and applications. *Biomaterials* **24**, 4337-4351 (2003).
3. Bodugoz-Senturk, H., Macias, C. E., Kung, J. H. & Muratoglu, O. K. Poly(vinyl alcohol)-acrylamide hydrogels as load-bearing cartilage substitute. *Biomaterials* **30**, 589-596 (2009).
4. Tanaka, Y., Fukao, K. & Miyamoto, Y. Fracture energy of gels. *Eur. Phys. J. E* **3**, 395-401 (2000).
5. Baumberger, T., Caroli, C. & Martina, D. Solvent control of crack dynamics in a reversible hydrogel. *Nat. Mater.* **5**, 552-555 (2006).
6. Naficy, S., Brown, H. R., Razal, J. M., Spinks, G. M. & Whitten, P. G. Progress toward robust polymer hydrogels. *Aust. J. Chem.* **64**, 1007–1025 (2011).
7. Haraguchi, K. & Takehisa, T. Nanocomposite hydrogels: a unique organic-inorganic network structure with extraordinary mechanical, optical, and swelling/de-swelling properties. *Adv. Mater.* **14**, 1120–1124 (2002).
8. Gong, J. P., Katsuyama, Y., Kurokawa, T. & Osada, Y. Double-network hydrogels with extremely high mechanical strength. *Adv. Mater.* **15**, 1155–1158 (2003).
9. Huang, T. *et al.* A novel hydrogel with high mechanical strength: a macromolecular microsphere composite hydrogel. *Adv. Mater.* **19**, 1622-1626 (2007).
10. Moutos, F. T., Freed, L. E. & Guilak, F. A biomimetic three-dimensional woven composite scaffold for functional tissue engineering of cartilage. *Nat. Mater.* **6**, 162-167 (2007).
11. Fung, Y. C. *Biomechanics: Mechanical Properties of Living Tissues*. (Springer-Verlag, New York, 2nd edition, 1993).
12. Gong, J. P. Why are double network hydrogels so tough? *Soft Matter* **6**, 2583-2590 (2010).
13. Na, Y. H. *et al.* Necking phenomenon of double-network gels. *Macromolecules* **39**, 4641-4645 (2006).
14. Webber, R. E., Creton, C., Brown, H. R. & Gong, J. P. Large strain hysteresis and Mullins effect of tough double-network hydrogels. *Macromolecules* **40**, 2919-2927 (2007).
15. Fantner, G. E. *et al.* Sacrificial bonds and hidden length dissipate energy as mineralized fibrils separate during bone fracture. *Nat. Mater.* **4**, 612-616 (2005).
16. Henderson, K. J., Zhou, T. C., Otim, K. J. & Shull, K. R. Ionically cross-linked triblock copolymer hydrogels with high strength. *Macromolecules* **43**, 6193-6201 (2010).
17. Haque, M. A., Kurokawa, T., Kamita, G. & Gong, J. P. Lamellar bilayers as reversible sacrificial bonds to toughen hydrogel: hysteresis, self-recovery, fatigue resistance, and crack blunting. *Macromolecules* **44**, 8916-8924 (2011).
18. Sun, J. Y. *et al.* Highly stretchable and tough hydrogels. *Nature* **489**, 133-136 (2012).
19. Higgs, P. G. & Joanny, J. F. Theory of polyampholyte solutions. *J. Chem. Phys.* **94**, 1543-1554 (1991).

20. Kudaibergenov, S. E. Recent advances in the study of synthetic polyampholytes in solutions. *Adv. Polym. Sci.* **144**, 115-197 (1999).
21. Nisato, G., Munch, J. P. & Candau, S. J. Swelling, structure, and elasticity of polyampholyte hydrogels. *Langmuir* **15**, 4236-4244 (1999).
22. Pafiti, K. S., Philippou, Z., Loizou, E., Porcar, L. & Patrickios, C. S. End-linked poly[2-(dimethylamino)ethyl methacrylate]-poly(methacrylic acid) polyampholyte conetworks: synthesis by sequential raft polymerization and swelling and sans characterization. *Macromolecules* **44**, 5352-5362 (2011).
23. Takeoka, Y. *et al.* First order phase transition and evidence for frustrations in polyampholytic gels. *Phys. Rev. Lett.* **82**, 4863-4865 (1999).
24. Zavitsas, A. A. Quantitative relationship between bond dissociation energies, infrared stretching frequencies, and force-constants in polyatomic molecules. *J. Phys. Chem.* **91**, 5573-5577 (1987).
25. Holyst, R. Some features of soft matter systems. *Soft Matter* **1**, 329-333 (2005).
26. Yu, Q. M., Tanaka, Y., Furukawa, H., Kurokawa, T. & Gong, J. P. Direct observation of damage zone around crack tips in double-network gels. *Macromolecules* **42**, 3852-3855 (2009).
27. Persson, B. N. J. & Brener, E. A. Crack propagation in viscoelastic solids. *Phys. Rev. E* **71**, 036123 (2005).
28. Varley, R. J., Shen, S. & van der Zwaag, S. The effect of cluster plasticisation on the self healing behaviour of ionomers. *Polymer* **51**, 679-686 (2010).
29. Nakajima, T. *et al.* True chemical structure of double network hydrogels. *Macromolecules* **42**, 2184-2189 (2009).
30. Bauer, A. M., Russell, A. P. & Shadwick, R. E. Mechanical properties and morphological correlates of fragile skin in gekkonid lizards. *J. Exp. Biol.* **145**, 79-102 (1989).
31. Taylor, D., O'Mara, N., Ryan, E., Takaza, M. & Simms, C. The fracture toughness of soft tissues. *J. Mech. Behav. Biomed. Mater.* **6**, 139-147 (2012).
32. Wang, Q. *et al.* High-water-content mouldable hydrogels by mixing clay and a dendritic molecular binder. *Nature* **463**, 339-343 (2010).
33. Nakahata, M., Takashima, Y., Yamaguchi, H. & Harada, A. Redox-responsive self-healing materials formed from host-guest polymers. *Nat. Commun.* **2**, 511-516 (2011).
34. Zhang, M. M. *et al.* Self-healing supramolecular gels formed by crown ether based host-guest interactions. *Angew. Chem. Int. Ed.* **51**, 7011-7015 (2012).
35. Cordier, P., Tournilhac, F., Soulié-Ziakovic, C. & Leibler, L. Self-healing and thermoreversible rubber from supramolecular assembly. *Nature* **451**, 977-980 (2008).
36. Tanaka, Y. *et al.* Determination of fracture energy of high strength double network hydrogels. *J. Phys. Chem. B* **109**, 11559-11562 (2005).
37. Rivlin, R. S. & Thomas, A. G. Rupture of rubber. I. Characteristic energy for tearing. *J. Polym. Sci.* **10**, 291-318 (1953).

Correspondence and requests for materials should be addressed to J. P. G.

### **Acknowledgements**

This research was financially supported by a Grant-in-Aid for Scientific Research (S) (No. 124225006) from the Japan Society for the Promotion of Science (JSPS). We thank Dr. T. Narita and Ms. M. Nargis for beneficial discussion.

### **Author contributions**

T. L. S., T. K., and J. P. G. designed the experiments. T. L. S., S. K., A. B. I., M. A. H., K. S., and T. A. performed the experiments. T. L. S., T. K., T. N., and J. P. G. analysed the data. T. L. S. and J. P. G. wrote the paper.

### **Additional information**

Supplementary information is available in the online version of the paper. Reprints and permissions information is available online at [www.nature.com/reprints](http://www.nature.com/reprints).

### **Competing financial interests**

The authors declare no competing financial interests.

## Figure legends

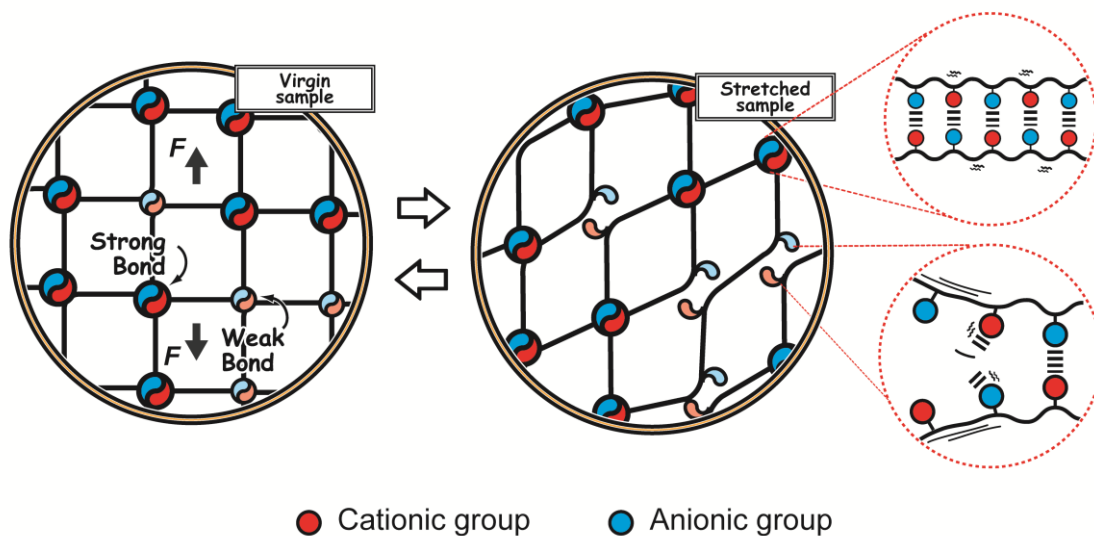
**Figure 1 Schematics of polyampholyte physical hydrogels.** **a**, Illustration of polyampholyte networks with ionic bonds of different strength. The strong bonds serve as permanent cross-linking points, and the weak bonds rupture under the deformation, as reversible sacrificial bonds. **b**, Chemical structures of monomers used in this work. Cationic monomer: 3-(methacryloylamino)propyl-trimethylammonium chloride (MPTC), methyl chloride quarternised *N,N*-dimethylamino ethylacrylate (DMAEA-Q); Anionic monomer: sodium *p*-styrenesulfonate (NaSS), 2-acrylamido-2-methylpropanesulfonic acid (AMPS).

**Figure 2 Effect of monomer concentration on the physical properties of polyampholytes.** **a**, Photographs of the polyampholytes P(NaSS-co-MPTC)  $C_m$ -0.52 polymerized with different total monomer concentrations  $C_m$ . Numbers in the images are the values of  $C_m$  (M). A single hydrogel phase is formed at  $C_m > 0.7$  M. **b**,  $C_m$  dependence of the swelling volume ratio  $Q_v$  and Young's modulus  $E$  of the polyampholyte hydrogels. **c**, Tensile behaviours of the polyampholyte hydrogels with different  $C_m$ . **d**, Dependence of the fracture stress  $\sigma_b$  and tearing energy  $T$  on the weight fraction of polymers  $C_{poly}$  of the polyampholyte hydrogels at the equilibrium swelling. Inset is a polarized microscope image of sample P(NaSS-co-MPTC) 2.1-0.52 being torn (white arrow indicates the crack tip front). All the error bars in this work represent standard deviations.

**Figure 3 Self-recovery, fatigue resistance, adhesion, and self-healing behaviours of polyampholyte hydrogels.** The data shown in **a**, **b**, **c**, **d**, and **e** are sample P(NaSS-co-MPTC) 2.1-0.52. **a**, Recovery of the sample for different waiting time performed by cyclic tensile test. **b**, Waiting time dependence of the residual strain and hysteresis ratio (area ratio of the second hysteresis loop to the first). **c**, Dependence of the area of hysteresis loop on the number of repeated cyclic tests for different loading strains. Recovery times are required between successive cyclic tests. **d**, Self-healing and adhesion between either two freshly cut surfaces (red and blue), or a fresh and an aged surface (white) of samples. **e**, Images demonstrating partial self-healing of the sample. **f**, Stress-strain curves of the virgin and self-healed sample P(NaSS-co-DMAEA-Q) 2.0-0.52. The self-healing in (**f**) is performed at 25 °C for 24 h in water, and others are indicated in text.

**Figure 4 Effect of saline solution and deformation-rate on properties of polyampholyte hydrogels P(NaSS-co-MPTC) 2.1-0.525.** **a**, Dependence of the swelling volume ratio  $Q_{salt,water}$  ( $= V_{salt}/V_{water}$ ) and Young's modulus  $E$  on the concentration of saline solution  $C_{NaCl}$  (M). The blue arrow indicates the physiological solution (0.15 M) condition. **b**, Tensile behaviours of the hydrogels after swelling in different concentration of saline solution  $C_{NaCl}$  (M). **c**, Tensile behaviours of the hydrogels under different deformation rate ranging from 5 to 900 mm/min. **d**, Deformation rate dependence of fracture stress  $\sigma_b$  and fracture strain  $\varepsilon_b$  of the hydrogels.

a



b

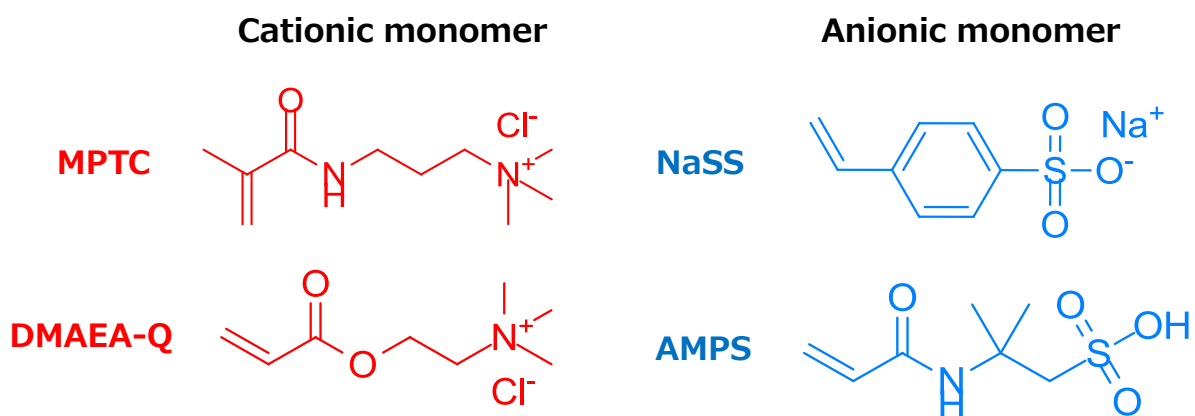


Figure 1 Schematics of polyampholyte physical hydrogels.

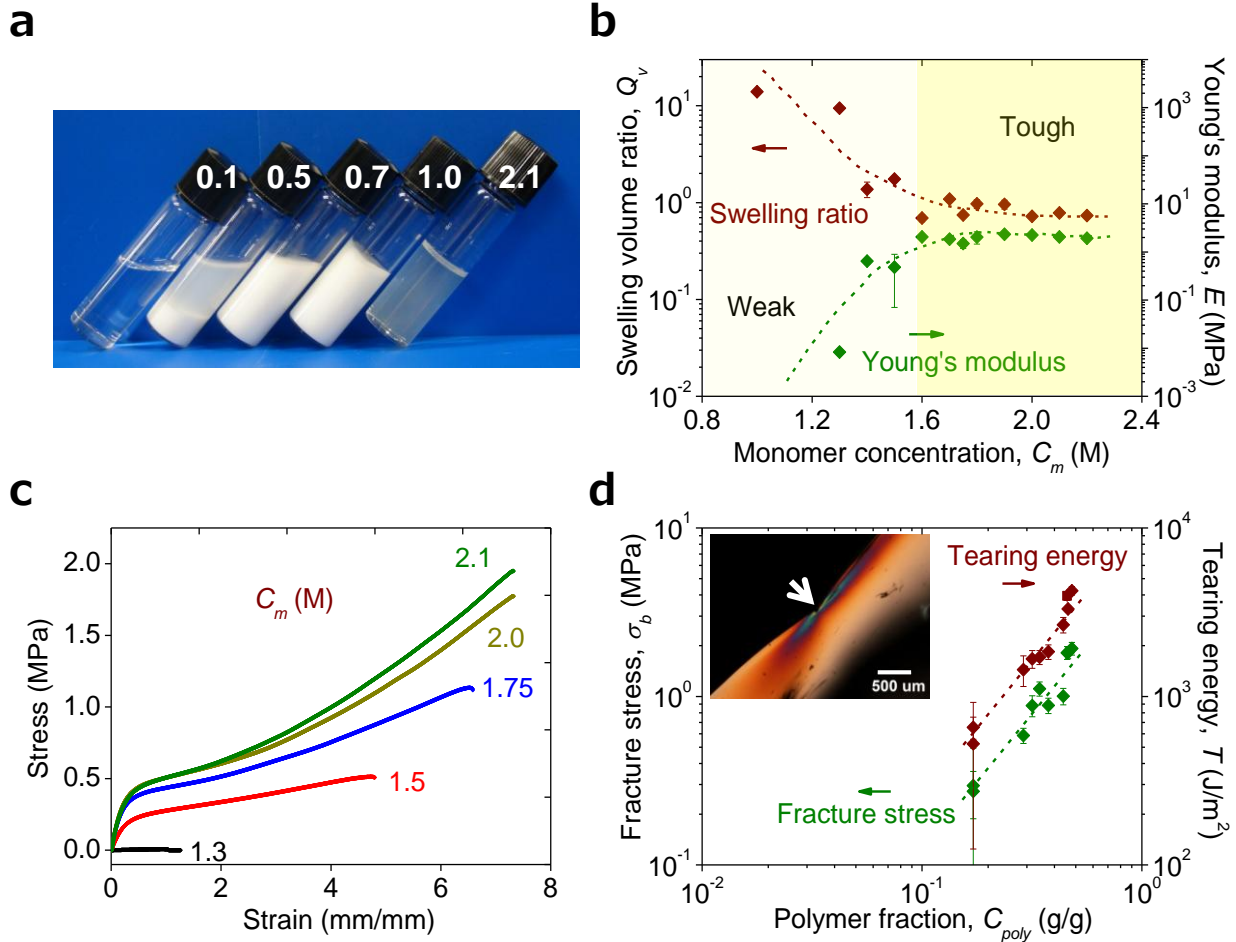


Figure 2 Effect of monomer concentration on the physical properties of polyampholytes

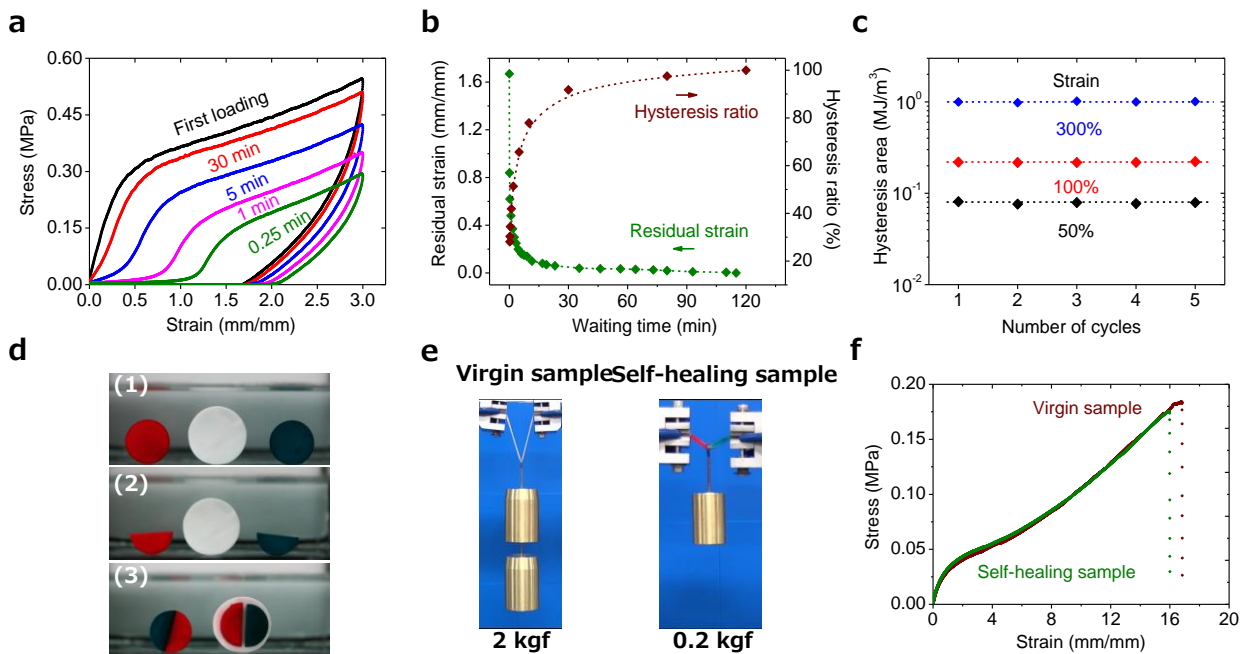


Figure 3 Self-recovery, fatigue resistance, adhesion, and self-healing behaviours of polyampholyte hydrogels.

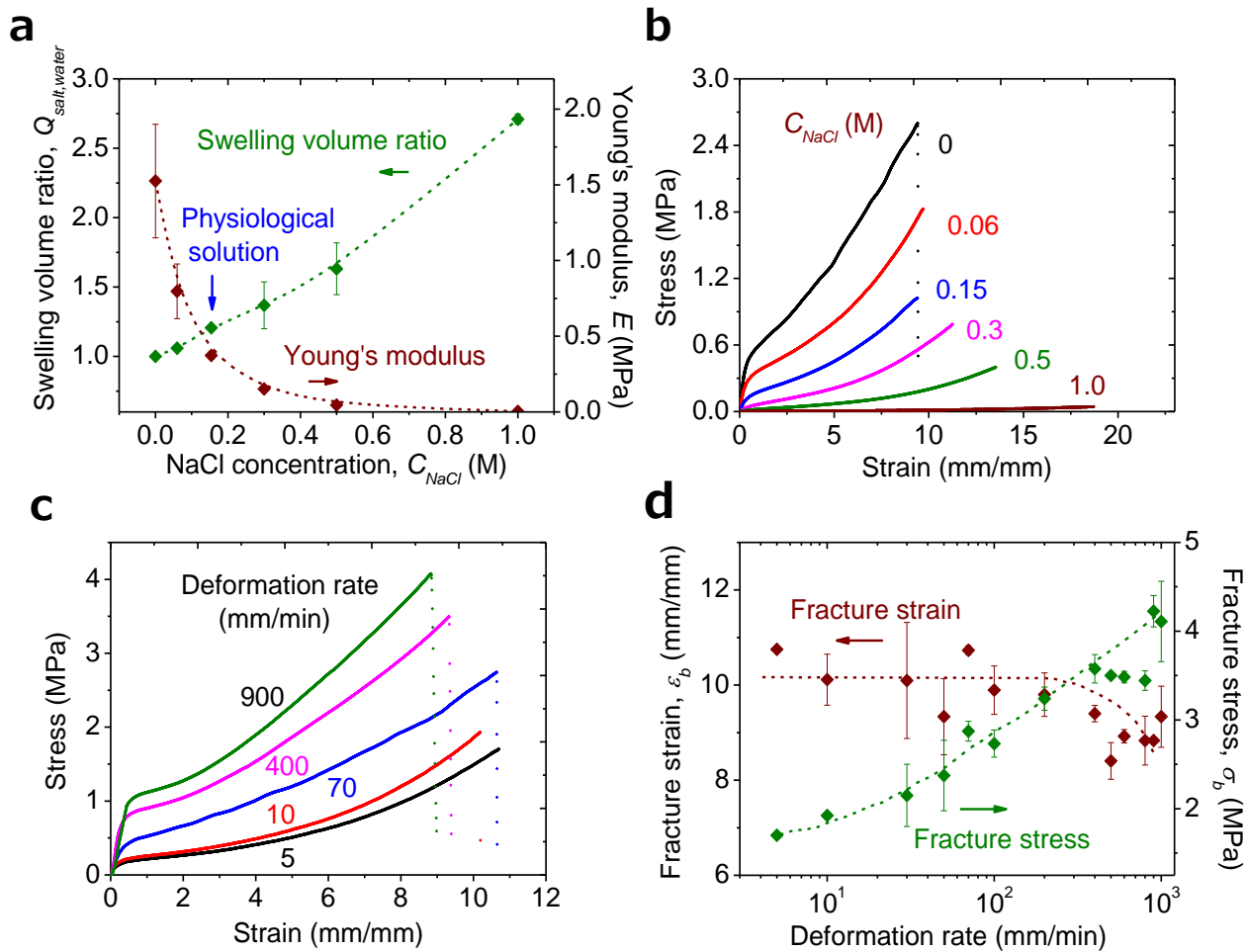


Figure 4 Effect of saline solution and deformation-rate on properties of polyampholyte hydrogels P(NaSS-co-MPTC) 2.1-0.525.